



This is a repository copy of *Synthesis of oligomeric and monomeric functionalized graphene oxides and a comparison of their abilities to perform as protein ligands and enzyme inhibitors*.

White Rose Research Online URL for this paper:
<https://eprints.whiterose.ac.uk/153284/>

Version: Published Version

Article:

Twyman, L.J. orcid.org/0000-0002-6396-8225 and Aziz, A. (2019) Synthesis of oligomeric and monomeric functionalized graphene oxides and a comparison of their abilities to perform as protein ligands and enzyme inhibitors. *ACS Applied Materials & Interfaces*, 11 (48). pp. 44941-44948. ISSN 1944-8244

<https://doi.org/10.1021/acsami.9b12980>

Reuse

This article is distributed under the terms of the Creative Commons Attribution (CC BY) licence. This licence allows you to distribute, remix, tweak, and build upon the work, even commercially, as long as you credit the authors for the original work. More information and the full terms of the licence here:
<https://creativecommons.org/licenses/>

Takedown

If you consider content in White Rose Research Online to be in breach of UK law, please notify us by emailing eprints@whiterose.ac.uk including the URL of the record and the reason for the withdrawal request.



eprints@whiterose.ac.uk
<https://eprints.whiterose.ac.uk/>

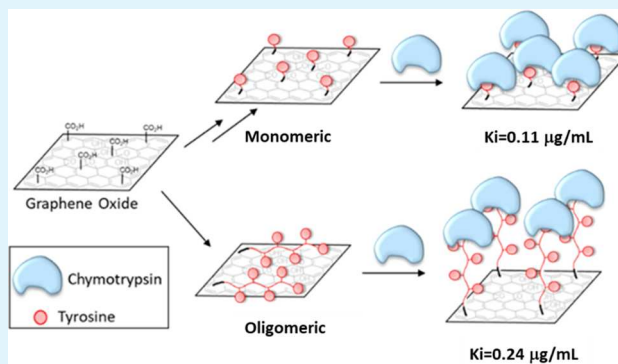
Synthesis of Oligomeric and Monomeric Functionalized Graphene Oxides and a Comparison of Their Abilities to Perform as Protein Ligands and Enzyme Inhibitors

Azrah Abdul Aziz and Lance J. Twyman*¹

Department of Chemistry, University of Sheffield, Sheffield S3 7HF, United Kingdom

Supporting Information

ABSTRACT: Graphene oxide (GO) is a versatile, monomolecular layered nanomaterial that possesses various oxygen-containing functionality on its large surface. These characteristics allow GO to interact with a variety of materials and to be applied towards a number of areas. The strength and selectivity of these interactions can be improved significantly through further functionalization. In this paper, we describe the functionalization of GO and its application as a protein ligand and an enzyme inhibitor. The work reported in this paper details how chymotrypsin inhibition can be improved using GO functionalized with a monomeric and oligomer layer of tyrosine. The results indicated that the mono- and oligo-functionalized systems performed extremely well, with K_i values nearly four times better than GO alone. Our original premise was that the oligomeric system would bind better because of the length of the oligomeric arms and potential for a high degree of flexibility. However, the results clearly showed that the shorter monomeric system was the better ligand/inhibitor. This was due to weaker intramolecular interactions between the aromatic side chains of tyrosine and the aromatic surface of GO. Although these are possible for both systems, they are cooperative and therefore stronger for the oligomeric functionalized GO. As such, the protein must compete and overcome these cooperative intramolecular interactions before it can bind to the functionalized GO, whereas the tyrosines on the surface of the monomeric system interact with the surface of GO through a significantly weaker monovalent interaction, but interact cooperatively with the protein surface.



KEYWORDS: graphene oxide, GO, functionalized graphene oxide, protein binding, enzyme inhibitor

INTRODUCTION

Graphene oxide (GO) and functionalized GO are important materials that can interact with other materials and be applied to a number of important areas. One such area is protein binding and enzyme inhibition. Most proteins function through cooperative partnerships with other proteins.¹ The complexes formed play essential roles in all biological processes and any unwanted or uncontrolled interactions can result in disease.² Modulating these interactions is central to drug design. Proteins recognize each other and other molecules through complementary functionalities positioned at precise points on large interacting surfaces, the key component of which is known as the “hot spot” or interfacial area.^{1,3} These surfaces involve specific interactions and range in size from 500 to 5000 Å.² Because of the size of these surfaces,^{4,5} it makes sense to design inhibitors and ligands that are large enough to interact fully with large interfacial binding areas. As such, there have been a number of approaches to study protein–ligand binding and/or inhibit protein–protein interactions using various macromolecules. These include calixarene and porphyrin scaffolds,^{6,7} nanomaterials,⁸ linear polymers,^{9,10}

and dendrimers.^{11,12} Graphene oxide has been shown to be an excellent material for protein binding.¹³ as it has a number of oxygen-containing functional groups on its surface, including carboxylic acids. Weight for weight, GO is currently the best ligand/inhibitor of the protein/enzyme chymotrypsin.¹³ In common with the macromolecules described above, GO possesses carboxylic acids that can interact with protein binding surfaces rich in cationic functionality. However, in addition to size and simple electrostatics, a number of other noncovalent interactions are important and these have a significant role with respect to selectivity (including charge/charge, hydrophobic, aromatic/ π – π interactions, and hydrogen bonding). In nature, these specific interactions come from a relatively narrow range of key amino acids. Studies have identified amino acids that contributed, on average, more than 2 kcal/mol to the binding energy, and only three amino acids were found to appear in interfacial areas with a frequency of

Received: July 23, 2019

Accepted: November 7, 2019

Published: November 7, 2019

more than 10%.¹⁴ These were amino acids capable of making multiple interactions and include tryptophan, 21%; arginine, 14%; and tyrosine, 13%. As such, multi/polyvalency, functionality, charge, and size are key design determinants with respect to obtaining selective ligands for protein binding. Therefore, changes in binding strength occur when functionalized macromolecules are used as protein ligands. These include functionalized porphyrins,¹⁵ linear polymers,¹⁶ and dendrimers.¹⁷

The aim of the work described within this paper was to determine whether or not the already significant protein binding ability of GO could be improved through functionalization. Of particular interest is functionalization with amino acids. One possible and simple way of achieving this is through the use of noncovalent chemistry. It is known that charged and aromatic amino acids can form relatively strong interactions with GO.¹⁸ However, in the presence of a protein, competition for amino acid binding between the GO and the protein results in a decreased interaction (due to a reduction in the number of multivalent interactions). Furthermore, previous studies to quantify binding (between GO and the amino acids) have reported that binding is relatively weak and takes place only at millimolar concentrations.¹⁹ As well as providing a level of robustness for any future applications, a covalent approach would allow much lower concentrations to be used. With regards to covalent approaches, there have been a number of reports describing the functionalization of GO with amino acids, including a recent paper describing a magnetic nanohybrid system for protein purification.²⁰ The most common method of functionalization describes the use of a coupling agent and an excess of amino acid in its *nonprotected* form.^{20–23} These methodologies produce a GO surface functionalized with an oligomeric amino acid surface. The process involves formation of an initial monomeric functionalized surface that goes on to react further with the excess amino acids. Alternatively, the unprotected amino acid reacts in solution to form dimers, trimers, and oligomers, which in turn add to the unfunctionalized or functionalized GO surface (where they are free to react further). Therefore, this methodology generates a functionalized GO surface with a random oligomeric layer of amino acids. In addition, as the aromatic amino acids important with respect to protein/enzyme binding tend to be aromatic,²⁴ the oligomeric chains will simply lay down and interact with the GO surface through favorable cooperative π – π interactions. As a result, these interactions must be broken and overcome before GO can bind to a protein surface. Additionally, the randomness and entropic freedom of the oligomeric chains could also lead to a lack of selectivity. Nevertheless, this simple method of functionalization may offer an advantage with respect to flexibility, resulting in high affinity and strong binding. In contrast, a monomeric layer of aromatic amino acids will bind to the surface of GO only through a single π – π interaction. Therefore, these monomeric interactions will be significantly weaker than the oligomer's cooperative interactions (with the GO surface). Consequently, it will be much easier for the monomeric amino acid system to interact with a protein surface. On the other hand, as the distance between the GO surface and the target protein could be much shorter for the monomeric system, there may be steric issues that could weaken binding. In addition, the lack of flexibility for the monomeric system could result in an improved selectivity.²⁵ It is also possible that neither will bind particularly well, and that

unfunctionalized GO is in fact the best ligand. Therefore, each system has advantages and disadvantages and an argument can be made for either with respect to protein binding. Without experimentation, it is not obvious which GO system will bind best to a target protein. To test this proposition, we proposed to functionalize the surface of GO with a monomeric and an oligomeric layer of tyrosine and to assess their binding affinities. Binding of the mono and oligo layered systems will be assessed relative to their ability to inhibit the activity of the protein α -chymotrypsin. Control experiments using unfunctionalized GO will also be carried out. Assessment of binding through inhibition experiments is possible, because the substrate entrance to the active site of α -chymotrypsin sits in the middle of its binding/interfacial area. Therefore, when GO binds, it blocks the active site entrance and the substrate cannot enter.¹² This will result in a reduction of the enzyme's activity, which can be used to assess relative binding efficiency.¹⁶ Kinetic data obtained using various substrate and GO concentrations will be used to determine kinetic parameters, including K_m , V_{max} , and K_i values, as well as determining the mode of binding.

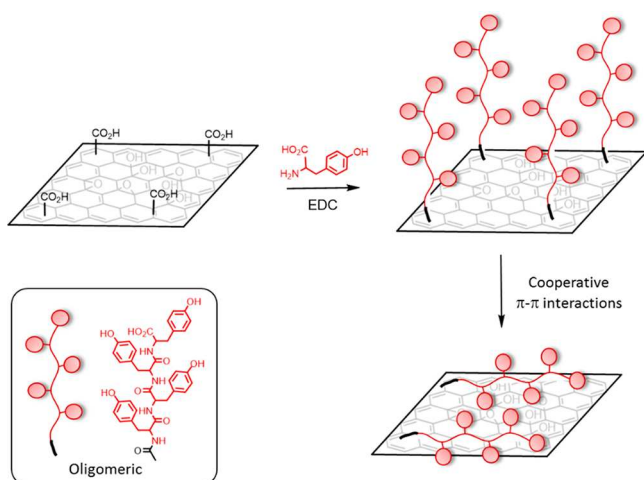
RESULTS AND DISCUSSION

Synthesis of Oligomeric and Monomeric Tyrosine Functionalized Graphene Oxide. Our aims were 2-fold. First, to test whether or not a functionalized GO would bind to protein surfaces with a higher affinity than GO alone. Second, we also wanted to determine whether the oligomeric or monomeric system bound with the greater affinity. To test our aims and methodology, we decided to functionalize GO with monomeric and oligomeric tyrosine. This amino acid possesses hydrophobic, π – π , and H-bonding interactions and can contribute more than 2 kcal/mol to the binding energy.¹⁴ Furthermore, tyrosine appears at the surface of proteins with a frequency of 13%, despite having a low overall frequency throughout protein structures. Tyrosine is therefore considered an important amino acid with respect to strong protein–protein binding.¹⁴

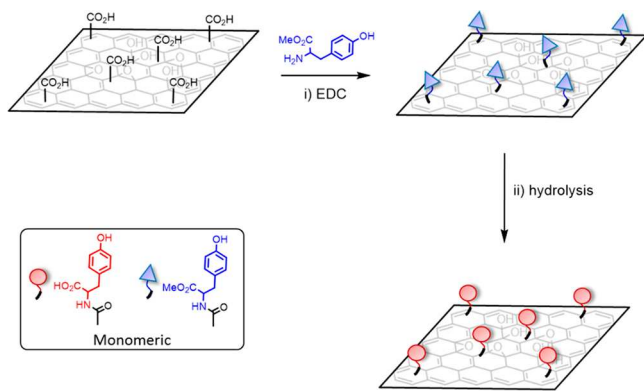
The graphene oxide required for our studies was synthesized using a variation of the Hummers method.²³ The structure of the GO obtained was confirmed by comparing its characterization data with published data (data provided in the [Supporting Information](#)).^{23,26–28} The next step was functionalization with a monomeric and oligomeric layer of amino acid. The oligomeric system was synthesized simply by adding EDC and nonprotected tyrosine to a suspension of GO in water and stirring for 24 h at 70 °C. The process is shown schematically in [Scheme 1](#). The monomeric system was synthesized using the same initial step, except that the methoxy ester of tyrosine was used. After isolation, the functionalized GO was resuspended in water and the ester group hydrolyzed using sodium hydroxide. A schematic representation of the two-step procedure is shown in [Scheme 2](#).

For the oligomeric system, peaks at 1582–1700 cm^{-1} corresponding to the C=O of amide and carboxylate groups, were visible in the FTIR spectrum. The NH stretching peak was observed at 3458 cm^{-1} . For the ester protected system, the C=O peak started around 1600 cm^{-1} , but extended to 1750 cm^{-1} , as a consequence of to the ester carbonyl stretch. In addition, no peaks corresponding to a carboxylic acid's OH stretch were visible (around 3000–3500 cm^{-1}). However, after deprotection, the OH peak returns to the spectrum, and the carbonyl peak no longer extends to the ester region (1750

Scheme 1. Synthesis of Oligomeric Tyrosine and Possible Binding on the Surface of GO



Scheme 2. Synthesis of a Monomeric Layer of Tyrosine on the Surface of GO, in Its Protected and Deprotected Forms



cm^{-1}), confirming hydrolysis of the ester protecting group. Elemental analysis provided further support for functionalization and also some information regarding the extent of functionalization. The carbon content increased from 40% for GO, to 45 and 48% for the monomeric and oligomeric systems, respectively. This increase in carbon content with an increasing level of functionalization is consistent with other reports.²¹ Elemental analysis also showed that nitrogen was present in both the monomeric and oligomeric systems, with a higher percentage observed for the oligomeric system (5.5% and 3% for the oligo and monomeric systems respectively). On its own, this does not necessarily indicate a higher level of functionalization, as this is dependent on the relative amounts of the other elements present. However, the carbon to nitrogen ratio can be used to assess qualitatively the relative levels of functionalization. A lower ratio indicates a higher proportion of nitrogen relative to the carbon content. The ratio for the two systems was 1:8 and 1:16 for the oligomeric and monomeric species respectively, confirming a higher level of functionalization for the oligomeric system. SEM-EDX mapping of the GO surface showed that only carbon and oxygen were present, whereas images for the monomeric and oligomeric samples also showed nitrogen (see the Supporting Information). Furthermore, quantitative SEM-EDX analysis indicated a carbon to nitrogen ratio of 1:4 for the oligomer and 1:10 for the monomer, which correlate reasonably well with elemental

analysis. TGA analysis of GO was identical to published data, with decomposition taking place in three phases. Initially, around 25% weight loss occurred at 50–120 °C, which was related to the loss of water. The second phase occurring between 120 and 440 °C corresponded to the loss of oxygen-containing groups and accounted for around 30% weight loss. The final phase took place between 440 and 750 °C (when the measurement was stopped) and is due to the pyrolysis of oxygen and unstable carbons remaining in the structure to yield CO and CO₂.^{25–27} The monomeric and oligomeric systems decomposed differently, with both showing the same initial degradation corresponding to loss of water. This was followed by a second decomposition from 100 to 600 °C (accounting for around 50% loss of weight) for the monomer. The oligomeric system was equally unstable, showing a continuous decomposition from 120 to 450 °C, which accounted for nearly 80% of the lost weight. For both systems, this was followed by a final pyrolysis stage from 600 to 750 °C. The different degradation behavior of the functionalized systems (with respect to GO) is a result of the amino acid and oligomer degradation,

RAMAN spectroscopy was used to identify the bond type/hybridization of the material, Figure 1. The RAMAN spectra of

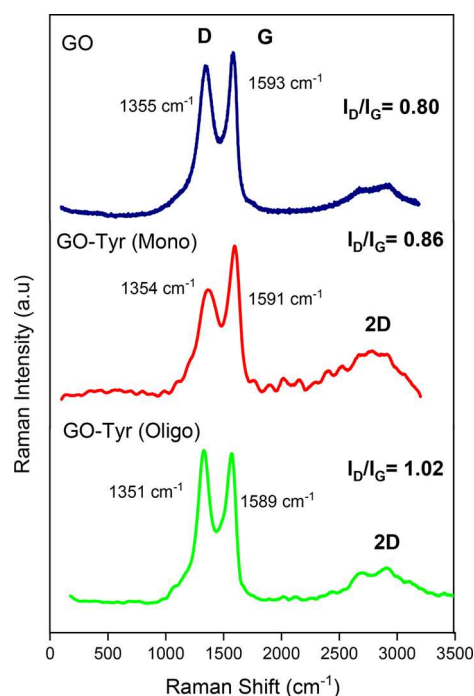


Figure 1. RAMAN spectra of GO and the oligomeric and monomeric tyrosine systems.

graphite has a single peak at 1575 cm^{-1} and this is associated with the sp^2 carbon bonds, Figure 1. As well as the sp^2 peak at 1593 cm^{-1} , GO also has a second peak at 1355 cm^{-1} , which is attributed to sp^3 atoms. These two peaks are often referred to as the G and D-bands, respectively, and the ratio of these two bands is an indicator of the level of functionalization. The I_D/I_G ratio for our GO was 0.80, which indicates a relatively high level of oxidation and generation of sp^3 atoms via the attachment of oxygen-containing functional groups.^{27–29} GO also has a broad peak at 2500–3200 cm^{-1} , which is referred to as the 2D band. The I_{2D}/I_G ratio can be used to estimate the number of GO layers.³⁰ In our case it was estimated that GO

sheets with less than five layers had formed.³¹ Functionalization of GO with tyrosine shifted the G and D bands to 1591 and 1352 cm^{-1} respectively. The I_D/I_G ratios for the monomeric systems increased to 0.86, which indicates an increased level of sp^3 atoms and further supports successful functionalization. For the oligomeric system, the I_D/I_G ratio increased further to 1.02, confirming an even greater extent of functionalization. XRD analysis of the functionalized systems showed that the original peak at 10° for GO, had shifted to 8.78° . The spectra also had a broad peak around 26° , which is consistent with an aromatic surface.^{32,33} The distance at the 2θ position was used to calculate the interlayer distance or d spacing. For the monomeric system this was measured as 0.86 nm, which is slightly higher than the 0.80 nm recorded for GO. This similarity is to be expected, as tyrosine is small and the aromatic functional groups are probably lying flat on the surface and minimizing the d spacing (as a result of π - π interactions). However, the d spacing for the oligomeric system was larger at 1.00 nm, which is greater than either the GO, or the monomeric functionalized system. Again, this to be expected as the oligomeric system is longer/bigger and will take up more space on the surface. Although the aromatic rings can lay flat on the surface, it is not necessarily true that all of the aromatic rings will, or can lay flat. This is particularly true for longer oligomers, where it is likely that “kinks” or “bulges” may form on the surface, which accounts for the higher d spacing.

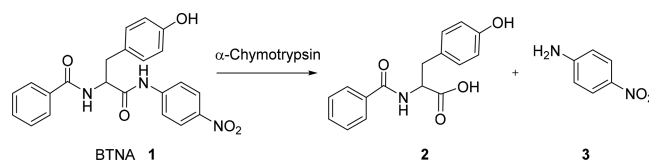
XPS was used to probe the electronic/bonding environment of various atoms. The N 1s XPS spectra showed two peaks, indicating two main bonding states of nitrogen (see the Supporting Information). The first, at a binding energy of 400.35 eV, is attributed to the nitrogen in the amide bond, which form when the amino acid reacts with the carboxylates on the surface (or the growing oligomer). The second peak comes at 400.7 eV and can be assigned to a nitrogen in an amine bond.^{23,34} The ratio of amide and amine peaks was 1 to 0.33 and 1 to 1.35, for the oligomer and monomer, respectively. This indicates that more amine bonds have formed in the monomeric system and this disparity comes from the differences in synthetic methods. During the synthesis, the N-terminus of the amino acid can react with the surface carboxylate groups to generate amides. However, the N-terminus can also react with the epoxides on the surface of GO to give an amine, and this is possible for both the oligomeric and monomeric synthesis. However, as a non-protected tyrosine is used in the oligomeric method, the N-terminus can also react with the C-terminus of another amino acid or a growing oligomer. Either will result in the formation of additional amide bonds, resulting in fewer amines; this is why the amide peak for the oligomeric system is much higher/more intense than the monomeric system. Overall, this supports our earlier assumption that oligomers form when nonprotected amino acids are used. Having synthesized and characterized the functionalized GO systems, we were now in a position to test their protein binding abilities.

Assessment of Protein Binding Using an Enzyme Inhibition Assay. Protein binding of the functionalized GO was assessed using an enzyme inhibition assay. The basic premise is based on the assumption that binding to the surface of an enzyme may prevent or reduce substrate access to the active site. This is particularly relevant for α -chymotrypsin whose active site entrance is rich in positive charge.³⁵ We have previously exploited this principle when demonstrating a size

based relationship between dendrimers and protein binding.^{17,36} De and Dravid used the same premise to demonstrate how unfunctionalized GO, which is rich in negative charge, could interact electrostatically with α -chymotrypsin.¹³ However, electrostatics are not the only interactions involved in protein binding. The active site entrance of α -chymotrypsin also contains functionality capable of engaging in a number of other interactions (e.g., H-bonding, π - π , and hydrophobic interactions).³⁷ Therefore, addition of complementary functionality to the surface of GO should result in improved selectivity. To test this, we carried out the hydrolysis of the enzyme substrate N-benzoyl tyrosine *p*-nitroanilide (BTNA), using α -chymotrypsin.

Upon hydrolysis, BTNA generates an aromatic species **3** that is yellow in color and can be used to follow the hydrolysis over time, Scheme 3. Initial rates can then be determined from plots

Scheme 3. Enzyme-Mediated Reaction Used to Assess Relative Binding to α -Chymotrypsin



of concentration versus time for the nitro aniline product **3**. Initially, a baseline/control was established for the activity of α -chymotrypsin in the absence of inhibitor, using BTNA as the substrate. The reactions were carried out using $2.0 \mu\text{M}$ BTNA and $0.4 \mu\text{M}$ α -chymotrypsin. The effect on the background rate for GO, the GO-Ty (mono) and GO-Ty (oligo), were determined by repeating the control experiment using α -chymotrypsin preincubated with $0.24 \mu\text{g/mL}$ of the specific inhibitor. For all experiments, the concentration of the hydrolysis product **3** was plotted against time, Figure 2. Initial velocities were obtained using Graphpad³⁸ and fitting the data using linear regression. Examination of the results (shown in Table 1) clearly indicate that all GO samples are effective inhibitors. With respect to the control, the unfunctionalized GO inhibited α -chymotrypsin by around 30%. The function-

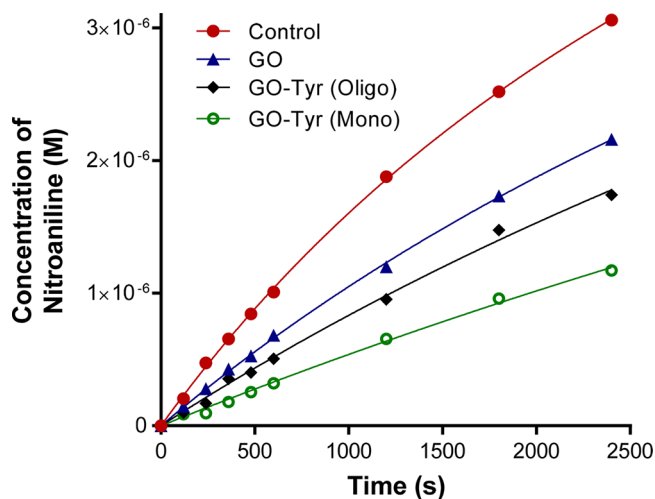


Figure 2. Rate plots used to determine the initial velocities (V) for the hydrolysis of the substrate BTNA ($2.0 \mu\text{M}$) using chymotrypsin ($0.4 \mu\text{M}$) in the presence and absence of GO inhibitors ($0.24 \mu\text{g/mL}$).

Table 1. Initial Rates Determined Using BTNA (2.0 μM), Chymotrypsin (0.4 μM), and Inhibitor (0.24 $\mu\text{g}/\text{mL}$)

| initial rate (nMs^{-1}) | inhibitor | | | |
|---------------------------------------|------------------------|------------------------|---------------------|------------------|
| | no inhibitor | GO | GO-Tyr (oligo) | GO-Tyr (mono) |
| 1.38 (± 0.06) | 0.95 (± 0.04) | 0.77 (± 0.04) | 0.51 (± 0.04) | |

alized GOs were even better inhibitors, with the monomeric system being the best. Specifically, at the concentrations used, the GO-Ty (mono) could inhibit more than 60% of the enzyme's activity relative to the control (uninhibited reaction).

To obtain more detailed inhibition and kinetic data, as well as establishing the mode of inhibition, initial rates for all species were determined at various inhibitor and substrate concentrations. The initial rates for various inhibitor and substrate concentrations are shown in Table 2. The initial rates

Table 2. Initial Rates Determined Using Various Concentrations of Substrate and Inhibitor^a

| | BTNA concentration (μM) | | | |
|---|--------------------------------------|------------------------|------------------------|------------------------|
| | 2.0 | 4.0 | 6.0 | 8.0 |
| control (0.0 $\mu\text{g}/\text{mL}$ GO) | 1.38 (± 0.06) | 2.23 (± 0.09) | 2.78 (± 0.01) | 3.24 (± 0.02) |
| GO 0.06 $\mu\text{g}/\text{mL}$ | 1.20 (± 0.50) | 2.10 (± 0.83) | 2.58 (± 0.90) | 3.87 (± 0.12) |
| GO 0.12 $\mu\text{g}/\text{mL}$ | 1.06 (± 0.44) | 1.89 (± 0.77) | 2.38 (± 0.96) | 2.70 (± 0.11) |
| GO 0.24 $\mu\text{g}/\text{mL}$ | 0.95 (± 0.04) | 1.69 (± 0.68) | 2.10 (± 0.86) | 2.41 (± 0.10) |
| GO 0.48 $\mu\text{g}/\text{mL}$ | 0.77 (± 0.03) | 1.40 (± 0.65) | 1.80 (± 0.78) | 2.12 (± 0.80) |
| GO-Tyr (oligo) 0.06 $\mu\text{g}/\text{mL}$ | 1.15 (± 0.48) | 1.94 (± 0.76) | 2.32 (± 0.97) | 2.76 (± 0.11) |
| GO-Tyr (oligo) 0.12 $\mu\text{g}/\text{mL}$ | 0.88 (± 0.04) | 1.74 (± 0.68) | 2.21 (± 0.93) | 2.42 (± 0.11) |
| GO-Tyr (oligo) 0.24 $\mu\text{g}/\text{mL}$ | 0.77 (± 0.04) | 1.48 (± 0.62) | 1.87 (± 0.75) | 2.17 (± 0.10) |
| GO-Tyr (oligo) 0.48 $\mu\text{g}/\text{mL}$ | 0.62 (± 0.01) | 1.12 (± 0.50) | 1.41 (± 0.65) | 1.73 (± 0.42) |
| GO-Tyr (mono) 0.06 $\mu\text{g}/\text{mL}$ | 1.07 (± 0.48) | 1.74 (± 0.78) | 2.16 (± 0.97) | 2.65 (± 0.12) |
| GO-Tyr (mono) 0.12 $\mu\text{g}/\text{mL}$ | 0.76 (± 0.42) | 1.44 (± 0.70) | 1.82 (± 0.89) | 2.11 (± 0.11) |
| GO-Tyr (mono) 0.24 $\mu\text{g}/\text{mL}$ | 0.51 (± 0.039) | 0.96 (± 0.06) | 1.27 (± 0.81) | 1.56 (± 0.94) |
| GO-Tyr (mono) 0.48 $\mu\text{g}/\text{mL}$ | 0.37 (± 0.03) | 0.71 (± 0.05) | 0.97 (± 0.07) | 1.17 (± 0.25) |

^aAll experiments conducted using 0.4 μM chymotrypsin.

obtained were then used to obtain Lineweaver–Burk plots and the result for the GO-Ty (mono) is shown in Figure 3 (top). The plots for all inhibitor concentrations share a common intercept, indicating that the mode of inhibition was a competitive inhibition (Lineweaver–Burk plots for the other systems are included within the Supporting Information). The initial rate data was subsequently plotted against the inverse of substrate concentration and the plots for each experiment fitted to a competitive inhibition model using eq 1 and Graphpad.³⁸ K_m is the Michaelis–Menten constant, V_{max} is the maximum enzyme velocity when saturated with substrate and K_i is the inhibition constant. S and I are the substrate and inhibitor concentrations, respectively.³⁹ Plots for the GO-Ty (mono) are shown in the bottom plot of Figure 3 (plots for

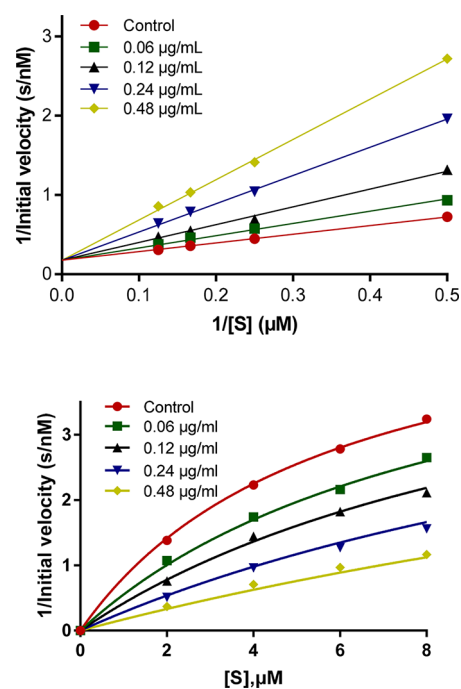


Figure 3. Top: Lineweaver–Burk plots that show a common intercept for all concentrations of GO-Tyr (mono) inhibitor, which indicate a competitive inhibition mechanism. Bottom: Plots of initial rate (Table 2) vs concentration of substrate (BTNA) at various concentrations of GO-Tyr (mono). The plots were fitted to a competitive inhibition model (eq 1 above and Graphpad), which produced values for K_i , K_m , and V_{max} . All experiments used a fixed concentration of chymotrypsin (0.4 μM).

the other systems are included within the Supporting Information).

$$V = \frac{V_{\text{max}}[S]}{K_m \left(1 + \frac{[I]}{K_i}\right) + [S]} \quad (1)$$

In all cases, the fit was excellent, returning R^2 values greater than 0.99, confirming that the mode of inhibition was a competitive process. The plots generated values for K_m and V_{max} values were similar in all cases and are shown in Table 3,

Table 3. Summary of Kinetic Parameters Obtained for All Graphene Oxide Inhibitors^a

| inhibitor | K_m | V_{max} | K_i $\mu\text{g}/\text{mL}$ |
|--------------|---------------------|---------------------|-------------------------------|
| GO | 5.61 (± 0.41) | 5.31 (± 0.19) | 0.40 (± 0.03) |
| GO-Tyr Oligo | 5.61 (± 0.58) | 5.28 (± 0.27) | 0.24 (± 0.02) |
| GO-Tyr Mono | 5.78 (± 0.53) | 5.50 (± 0.25) | 0.11 (± 0.02) |

^aData obtained from initial velocity vs substrate concentration and subsequent fits to a competitive inhibition model (Graphpad).

along with the K_i values. The K_i value is a measure of the concentration required to inhibit the activity by 50%. Our data clearly indicate that the functionalized GO systems are better inhibitors than GO alone. As inhibition is related to binding, we can also conclude that the functionalized GO systems bind to the protein surface more strongly than unfunctionalized GO, resulting in enhanced inhibition. The strongest inhibitor was the GO-Ty (mono), which had a K_i of 0.11 $\mu\text{g}/\text{mL}$. This was more than 200% better than the oligomeric system and nearly 400% better than GO alone. Overall, the data confirmed

that that a GO surface functionalized with a monomeric layer of tyrosine binds and inhibits the activity of chymotrypsin the best.

Having established that GO functionalized with monomeric or oligomeric layers of tyrosine could outperform GO as an enzyme inhibitor, we next needed to confirm that inhibition occurred through our proposed binding mechanism and that inhibition was *not* due to denaturation or any changes in protein structure (caused by GO binding). This was achieved using similar methods to those previously used to study the effect of macro-ligand binding to the surface of proteins.^{40,41} Specifically, CD spectroscopy was used to record spectra of chymotrypsin in the presence and absence of the functionalized GO systems. The spectra were then compared to each other to determine whether or not binding to the protein's surface resulted in changes to the secondary structure. Experiments were carried out after a 1 h incubation and concentrations of 0.4 μM and 0.48 $\mu\text{g/mL}$ for the protein and GO systems, respectively. All measurements were carried out at 37 $^{\circ}\text{C}$ and at pH 7.35. The spectra obtained, which are shown in Figure 4, clearly show that none of the GO systems

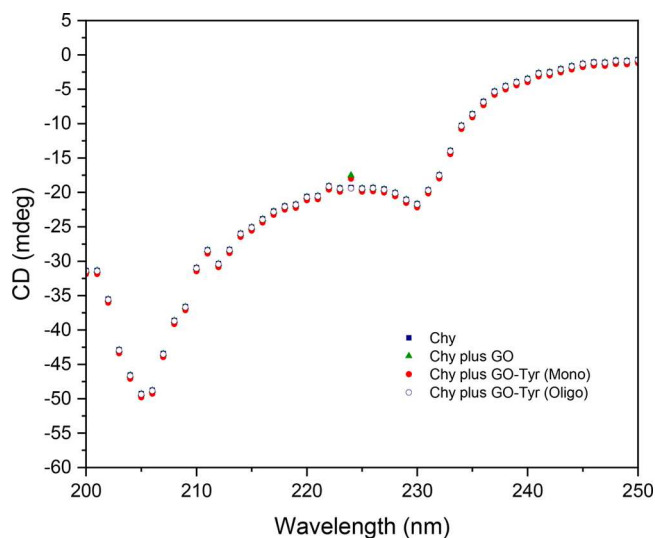


Figure 4. CD spectra for chymotrypsin and complexes of chymotrypsin with GO, GO-Tyr (mono), and GO-Tyr (oligo).

have any effect on the spectra, and therefore no effect on the structure of the protein. The experiments were repeated after 24 and 36 h, and no changes in the spectra were observed. Therefore, the GO systems inhibit enzymatic activity without denaturing the protein. This means that the GO sheets are able to adapt their structure sufficiently to match the surface curvature of the protein.⁴² As well as monitoring the structures over time, we also studied the effect of heat on the structure of Chy in the presence and absence of the GO.^{40,41} Experiments were performed at the same concentrations and pH (described above). The samples were heated up and the intensity of the peak at 224 nm monitored with respect to temperature. The results indicated no differences in the extent of denaturation with respect to temperature, generating identical plots for all GO systems. Therefore, binding of the GO systems did not destabilize or stabilize the protein structures. This result is similar to that obtained using functionalized and unfunctionalized dendrimers.¹¹

CONCLUSIONS

Although it was known that graphene oxide could bind strongly to the surface of proteins, we wanted to determine if a functionalized GO could bind proteins more strongly than a corresponding unfunctionalized GO. In addition to improving binding, it may also be possible (in the future) to introduce selectivity via functionalization. The functionality selected for our initial study was the amino acid tyrosine. Tyrosine is one of the few amino acids known to be important with respect to protein–protein binding and protein–surface binding. In addition to determining how a specific functional group may influence binding, we wanted to know if the extent and specific levels of functionalization (in regards of surface thickness and any spacer effect provided by the oligomer) was an important parameter with respect to protein binding. As such, we successfully synthesized graphene oxide with an oligomeric layer of tyrosine using nonprotected tyrosine and an EDC coupling methodology. A monomeric functionalized graphene oxide was also synthesized using a simple two-step procedure. The first involved the same EDC-mediated addition of C-protected tyrosine, with a second step required to hydrolyze and remove the protecting groups. All of the GO systems were able to inhibit the function of chymotrypsin. Kinetic analysis indicated that the monomeric system inhibited the best and therefore bound the strongest, with a K_i value of 0.11 $\mu\text{g/mL}$. This is almost four times better than GO alone (K_i 0.40 $\mu\text{g/mL}$) and double the affinity of the oligomeric functionalized GO (K_i 0.24 $\mu\text{g/mL}$). In addition, the kinetic analysis confirmed all systems bound and inhibited chymotrypsin via the same competitive binding mechanism. As such, any differences in binding affinity/inhibition are not related to differences in the mode or mechanism of binding. When analyzing the reasons for the differences in binding affinity, we conclude that the oligomeric system binds and inhibits less well (than the monomeric functionalized GO), due to unfavorable cooperative interactions between the aromatic units of the oligomeric chain and the graphene oxide surface. Consequently, protein binding is in competition with this strong intramolecular binding, which must be overcome before the amino acids can bind to the protein surface. Although the same intramolecular interactions occur for the monomeric system, they are unimolecular and not cooperative. As a result, the intramolecular interaction between the amino acids and GO are much weaker and can be easily broken by the protein when binding to the amino acids through stronger intermolecular cooperative interactions. Therefore, when designing GO-based systems for selective protein or polyvalent binding (or any application requiring strong and/or selective binding to GO), it is important to take into account any intramolecular cooperative effects involving the GO surface, as these will weaken any intermolecular interactions. Overall, we have demonstrated that functionalized GO can bind to chymotrypsin with high affinity and this affinity can be moderated by the level of oligomerization. In an effort to obtain new protein ligands and enzyme inhibitors that are more selective with respect to their binding, we are currently exploiting the methodology and results to design and construct new GO inhibitors.

METHODS AND MATERIALS

Instrumentation. *RAMAN Spectrometer.* Samples were recorded from 500 to 3500 cm^{-1} on a Renishaw inVianRaman Microscope using a green laser operating at wavelength of 514.5 nm and laser

power at 20 mV. X-ray photoelectron spectrometry (XPS) measurements were performed using monochromatic Al- $k\alpha$ radiation ($h\nu = 1486.69$ eV). CasaXPS v 2.3.16 software was used to perform curve fitting and to calculate the atomic concentrations. Thermogravimetric analysis (TGA) was performed using a PerkinElmer Pyris in the range of 25 °C - 800 °C. Origin 2018 software was used to analyze the data. X-ray diffractometer (XRD) patterns were collected using a Bruker, D8 Advanced diffractometer with a copper target at the wavelength of λ CuK $\alpha = 1.54178$ Å and a tube voltage of 40 kV and tube current of 35 mA, in the range of 5–100° at the speed of 0.05°/min. Elemental Analysis (EA) performed using a Vario MICRO Cube and solid powder was used. Scanning electron microscope (SEM) samples were analyzed by a JEOL-7001F operated at 15 kV. Dry powder was used for the SEM and EDX analysis. CD spectra were recorded on a Jasco spectropolarimeter model J-810, equipped with Peltier temperature-controller. A Quartz cell of 1 cm path-length was used. Spectra were measured at 50 nm/min, 0.5 nm of data pitch, 1 s of response, and a bandwidth of 1 nm. The CD spectrum was recorded in millidegrees of ellipticity as a function of wavelength. Spectral resolution between two consecutive ellipticity readings is 0.5 nm. Solutions were carried out at pH 7.35 and concentrations of 0.4 μ M and 0.48 μ g/mL for the protein and GO systems, respectively. CD spectrum were obtained at 37 °C. The effects of temperature on protein structure were determined by recording spectra at 1 °C intervals from 37 to 95 °C (spectra recorded at 224 nm).

Synthesis. Graphene Oxide (GO). Graphite flakes (3.0 g, 1.0 equiv.) were mixed to a 9:1 mixture of concentrated H₃PO₄/ H₂SO₄ (40:360 mL) and added to 18.0 g of KMnO₄ (6.0 equiv.), a slight exotherm (around 40 °C) was produced. The reaction was stirred at 50 °C for 24 h. The reaction was allowed to cool at room temperature and the mixture poured onto ice (500 mL), before 3 mL of 30% H₂O₂ was added. The crude product was centrifuged (4000 rpm, 30 min) and the supernatant decanted away. The crude product was then washed several times with water (400 mL), 30% HCl (400 mL), and ethanol (400 mL). Ether (400 mL) was then added to aid coagulation and the suspension collected by filtered. The solids were vacuum-dried for 24 h at room temperature. The product (4.1 g) was obtained as a dark brown solid.

Graphene Oxide Tyr-OCH₃ (methyl ester). GO (0.20 g) was dispersed in deionized water (100 mL) and sonicated with ultrasonic oscillation for 3 h. L-Tyrosine methyl ester (2.0 g, 12 mmol), DMAP (2.93 g, 24.0 mmol), triethylamine (3.67 g, 36.0 mmol), and EDC.HCl (4.64 g, 24.0 mmol) were added. The mixture was stirred at 75 °C for 24 h. The reaction was allowed to cool to room temperature and the solids collected by filtration. The solid was washed with brine (100 mL \times 3) and the filtrate centrifuged for 45 min (at 4000 rpm). The precipitates produced were washed again with water and ethanol and dried at 60 °C. The product (0.34 g) was obtained as a black solid.

Graphene Oxide Tyr (mono-deprotection). GO (0.20 g) was dispersed in 100 mL of deionized water and was sonicated with ultrasonic oscillation for 4 h. The mixture was mixed with 20 mL of KOH (2 M) and stirred at 75 °C for 24 h. The reaction mixture was allowed to cool to room temperature. 20 mL of sulfuric acid (2 M) was added and the mixture sonicated with ultrasonic oscillation for 4 h. The solid was washed with brine solution (100 mL \times 4), collected by filtration and dried in a vacuum oven at 60 °C overnight. The product (0.33 g) was obtained as a black powder.

Graphene Oxide - Tyr (Oligo). GO (0.20 g) was dispersed in deionized water (100 mL) and sonicated with ultrasonic oscillation for 4 h. Excess L-tyrosine (10 g) and DMAP (2.93 g, 24.0 mmol), triethylamine (3.67 g, 36.0 mmol), and EDC-HCl (4.64 g, 24.0 mmol) were added. The reaction mixture was stirred at 75 °C for 24 h. The reaction mixture was allowed to cool at room temperature and the solids collected and washed with brine (100 mL \times 4). The filtrate was centrifuged for 45 min (4000 rpm) and the supernatant produced was decanted away. The solids were washed with water and ethanol. The product was dried in a vacuum oven at 60 °C overnight to yield the product (0.31 g) as a black solid.

Kinetic Studies. Assay of GO-Chymotrypsin Activity. The enzyme activity was measured at a BTNA (substrate) concentrations of 2.0, 4.0, 6.0, and 8.0 μ M and concentrations of GO/functionalized GO of 0.0, 0.06, 0.12, 0.24, and 0.48 μ M. All experiments were performed at an enzyme concentration of 0.4 μ M. Initial velocity for each GO/substrate combination was obtained by linear fittings of 4-nitroaniline production over time using Graphpad prism 7.0. All measurements were recorded at least three times. The data obtained was plotted as Lineweaver–Burk plots to establish the mode of inhibition. The initial rate data was subsequently replotted with respect to inverse substrate concentration and the plot fitted using a competitive inhibition model (using Graphpad 7.0).

■ ASSOCIATED CONTENT

📄 Supporting Information

The Supporting Information is available free of charge on the ACS Publications website at DOI: 10.1021/acsami.9b12980.

Characterization data of the functionalized systems including elemental data, SEM-EDX, XRD, IR and Raman, XPS. and CD; plots used to obtain the kinetic data for the GO and GO-Tyr (oligo) (PDF)

■ AUTHOR INFORMATION

Corresponding Author

*Email: l.j.twyman@sheffield.ac.uk

ORCID

Lance J. Twyman: 0000-0002-6396-8225

Notes

The authors declare no competing financial interest.

■ ACKNOWLEDGMENTS

The authors thank Majlis Amanah Rakyat (MARA) for funding a scholarship (A.A.).

■ REFERENCES

- (1) Jones, S.; Thornton, J. M. Principles of Protein-Protein Interactions. *Proc. Natl. Acad. Sci. U. S. A.* **1996**, *93*, 13–20.
- (2) Ryan, D. P.; Matthews, J. M. Protein-Protein Interactions in Human Disease. *Curr. Opin. Struct. Biol.* **2005**, *15*, 441–446.
- (3) Keskin, O.; Gursoy, A.; Ma, B.; Nussinov, R. Principles Of Protein-Protein Interactions: What Are the Preferred Ways for Proteins to Interact? *Chem. Rev.* **2008**, *108*, 1225–1244.
- (4) Chothia, C.; Janin, J. Principles of Protein-Protein Recognition. *Nature* **1975**, *256*, 705–708.
- (5) Reichmann, D.; Rahat, O.; Cohen, M.; Neuvirth, H.; Schreiber, G. The Molecular Architecture of Protein-Protein Binding Sites. *Curr. Opin. Struct. Biol.* **2007**, *17*, 67–76.
- (6) Park, H.; Lin, Q.; Hamilton, A. Modulation of Protein–Protein Interactions by Synthetic Receptors: Design of Molecules that Disrupt Serine Protease–Proteinaceous Inhibitor Interaction. *Proc. Natl. Acad. Sci. U. S. A.* **2002**, *99*, 5105–5109.
- (7) Yin, H.; Hamilton, A. D. Strategies For Targeting Protein-Protein Interactions with Synthetic Agents. *Angew. Chem., Int. Ed.* **2005**, *44*, 4130–4163.
- (8) Kim, J. K.; Yang, S. Y.; Lee, Y.; Kim, Y. Functional Nanomaterials Based on Block Copolymer Self-Assembly. *Prog. Polym. Sci.* **2010**, *35*, 1325–1349.
- (9) Welsch, N.; Dzubiella, J.; Graebert, A.; Ballauff, M. Protein Binding to Soft Polymeric Layers. *Soft Matter* **2012**, *8*, 12043–12052.
- (10) Wei, Q.; Becherer, T.; Angioletti-Uberti, S.; Dzubiella, J.; Wischke, C.; Neffe, A. T.; Lendlein, A.; Ballauff, M.; Haag, R. Protein Interactions with Polymer Coatings and Biomaterials. *Angew. Chem., Int. Ed.* **2014**, *53*, 8004–8031.

- (11) Chiba, F.; Hu, T. C.; Twyman, L. J.; Wagstaff, M. Dendrimers as Size Selective Inhibitors to Protein-Protein Binding. *Chem. Commun.* **2008**, 4351–4353.
- (12) Chiba, F.; Mann, G.; Twyman, L. J. Investigating Possible Changes in Protein Structure During Dendrimer-Protein Binding. *Org. Biomol. Chem.* **2010**, *8*, 5056–5058.
- (13) De, M.; Chou, S. S.; Dravid, V. P. Graphene Oxide as an Enzyme Inhibitor: Modulation of Activity of f-Chymotrypsin. *J. Am. Chem. Soc.* **2011**, *133*, 17524–17527.
- (14) Bogan, A. A.; Thorn, K. S. Anatomy of Hot Spots in Protein Interfaces. *J. Mol. Biol.* **1998**, *280*, 1–9.
- (15) Baldini, L.; Wilson, A. J.; Hong, J.; Hamilton, A. D. Pattern-Based Detection of Different Proteins Using an Array of Fluorescent Protein Surface Receptors. *J. Am. Chem. Soc.* **2004**, *126*, S656–S657.
- (16) Wenck, K.; Koch, S.; Renner, C.; Sun, W.; Schrader, T. A Noncovalent Switch for Lysozyme. *J. Am. Chem. Soc.* **2007**, *129*, 16015–16019.
- (17) Chiba, F.; Twyman, L. J. Effect of Terminal-Group Functionality on the Ability of Dendrimers to Bind Proteins. *Bioconjugate Chem.* **2017**, *28*, 2046–2050.
- (18) Li, S.; Aphale, A. N.; Macwan, I. G.; Patra, K. P.; Gonzalez, W. G.; Miksovskaja, J.; Leblanc, R. M. Graphene Oxide as a Quencher for Fluorescent Assay of Amino Acids, Peptides, and Proteins. *ACS Appl. Mater. Interfaces* **2012**, *4*, 7069–7075.
- (19) Pandit, S.; De, M. Interaction of Amino Acids and Graphene Oxide: Trends in Thermodynamic Properties. *J. Phys. Chem. C* **2017**, *121*, 600–608.
- (20) Yan, M.; Liang, Q.; Wan, W.; Han, Q.; Tan, S.; Ding, M. Amino Acid-Modified Graphene Oxide Magnetic Nanocomposite for the Magnetic Separation of Proteins. *RSC Adv.* **2017**, *7*, 30109–30117.
- (21) Mallakpour, S.; Abdolmaleki, A.; Borandeh, S. Fabrication of Amino Acid-Based Graphene-Zinc Oxide (Zno) Hybrid and its Application for Poly(Ester-Amide)/Graphene-Zno Nanocomposite Synthesis. *J. Thermoplast. Compos. Mater.* **2017**, *30*, 358–380.
- (22) Rambabu, G.; Bhat, S. D. Amino Acid Functionalized Graphene Oxide Based Nanocomposite Membrane Electrolytes for Direct Methanol Fuel Cells. *J. Membr. Sci.* **2018**, *551*, 1–11.
- (23) González-Domínguez, J. M.; Gutiérrez, F. A.; Hernández-Ferrer, J.; Ansón-Casaos, A.; Rubianes, M. D.; Rivas, G.; Martínez, M. T. Peptide-Based Biomaterials. Linking L-Tyrosine and Poly L-Tyrosine to Graphene Oxide Nanoribbons. *J. Mater. Chem. B* **2015**, *3*, 3870–3884.
- (24) Vovusha, H.; Sanyal, S.; Sanyal, B. Interaction of Nucleobases and Aromatic Amino Acids with Graphene Oxide and Graphene Flakes. *J. Phys. Chem. Lett.* **2013**, *4*, 3710–3718.
- (25) Weber, F.; Brune, S.; Borgel, F.; Lange, C.; Korpis, K.; Bednarski, P. J.; Laurini, E.; Fermeglia, M.; Priel, S.; Schepmann, D.; Wunsch, B. Rigidity versus Flexibility: Is This an Issue in $\sigma 1$ Receptor Ligand Affinity and Activity? *J. Med. Chem.* **2016**, *59* (11), 5505–5519.
- (26) Marcano, D.; Kosynkin, D.; Berlin, J.; Sinitskii, A.; Sun, Z.; Slesarev, A.; Alemany, L. B.; Lu, W.; Tour, J. M. Improved Synthesis of Graphene Oxide. *ACS Nano* **2010**, *4*, 4806–4814.
- (27) Wall, M. *Thermo Scientific Application Note S2252: The Raman Spectroscopy Of Graphene and the Determination of Layer Thickness*; Thermo Fisher Scientific, 2011.
- (28) Kuilla, T.; Bhadra, S.; Yao, D.; Kim, N. H.; Bose, S.; Lee, J. H. Recent Advances in Graphene Based Polymer Composites. *Prog. Polym. Sci.* **2010**, *35*, 1350–1375.
- (29) Kumar, P.; Kanaujia, P. K.; Vijaya Prakash, G.; Dewasi, A.; Lahiri, I.; Mitra, A. Growth Of Few- and Multilayer Graphene on Different Substrates Using Pulsed Nanosecond Q-Switched Nd:YAG Laser. *J. Mater. Sci.* **2017**, *52*, 12295–12306.
- (30) Graf, D.; Molitor, F.; Ensslin, K.; Stampfer, C.; Jungen, A.; Hierold, C.; Wirtz, L. Spatially Resolved Raman Spectroscopy of Single and Few-Layer Graphene. *Nano Lett.* **2007**, *7*, 238–242.
- (31) Pan, B.; Cui, D.; Gao, F.; He, R. Growth of Multi-Amine Terminated Poly(Amidoamine) Dendrimers on the Surface Of Carbon Nanotubes. *Nanotechnology* **2006**, *17*, 2483–2489.
- (32) Mallakpour, S.; Abdolmaleki, A.; Borandeh, S. Covalently Functionalized Graphene Sheets with Biocompatible Natural Amino Acids. *Appl. Surf. Sci.* **2014**, *307*, 533–542.
- (33) Kumar, M.; Swamy, B. E. K.; Asif, M. H. M.; Viswanath, C. C. Preparation of Alanine and Tyrosine Functionalized Graphene Oxide Nanoflakes and their Modified Carbon Paste Electrodes for the Determination of Dopamine. *Appl. Surf. Sci.* **2017**, *399*, 411–419.
- (34) Meng, H.; Sui, G. X.; Fang, P. F.; Yang, R. Effects of Acid- and Diamine-Modified Mwnts on the Mechanical Properties and Crystallization Behavior of Polyamide. *Polymer* **2008**, *49*, 610–620.
- (35) Hedstrom, L. Serine Protease Mechanism and Specificity. *Chem. Rev.* **2002**, *102*, 4501–4523.
- (36) Chiba, F.; Hu, T. C.; Twyman, L. J.; Wagstaff, M. Dendrimers as Size Selective Inhibitors to Protein-Protein Binding. *Chem. Commun.* **2008**, 4351–4353.
- (37) Copeland, R. A. *Evaluation of Enzyme Inhibitors in Drug Discovery: A Guide for Medicinal Chemists and Pharmacologists*; John Wiley and Sons, 2005; pp 25–55.
- (38) Copeland, R. A. *Enzymes: A Practical Introduction to Structure, Mechanism, and Data Analysis*; Wiley-Blackwell: 2001; p 278.
- (39) Segel, I. H. *Enzyme Kinetics: Behavior and Analysis of Rapid Equilibrium and Steady-State Enzyme Systems*; Wiley-Interscience: 1993.
- (40) Cai, J.; Rosenzweig, B. A.; Hamilton, A. D. Inhibition of Chymotrypsin by a Self-Assembled DNA Quadruplex Functionalized with Cyclic Peptide Binding Fragments. *Chem. - Eur. J.* **2009**, *15*, 328–332.
- (41) Chiba, F.; Mann, G.; Twyman, L. J. Investigating possible changes in protein structure during dendrimer–protein binding. *Org. Biomol. Chem.* **2010**, *8*, 5056–5058.
- (42) Dobson, C. M. The Fundamental Mechanism of Protein Folding. *Nature* **2003**, *426*, 884–890.